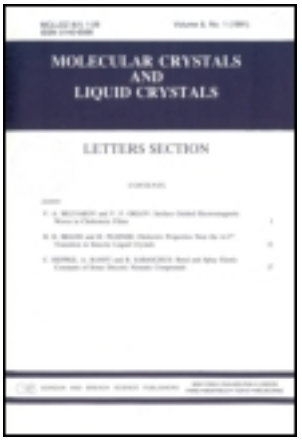

Molecular Crystals and Liquid Crystals
Publication details, including instructions for authors and subscription information:
http://www.tandfonline.com/loi/gmcl20

Studies on Pressure-Dependent Electrical Resistivity of $MoSe_{2-x}Te_x$ Single Crystals

D. N. Bhavsar [a] & A. R. Jani [a]
[a] High Pressure Laboratory, Department of Physics , Sardar Patel University , Vallabh Vidyanagar , Gujarat , India
Published online: 16 Dec 2013.

To cite this article: D. N. Bhavsar & A. R. Jani (2013) Studies on Pressure-Dependent Electrical Resistivity of $MoSe_{2-x}Te_x$ Single Crystals, Molecular Crystals and Liquid Crystals, 587:1, 121-128, DOI: 10.1080/15421406.2013.821646

To link to this article: http://dx.doi.org/10.1080/15421406.2013.821646

Mol. Cryst. Liq. Cryst., Vol. 587: pp. 121–128, 2013

ISSN: 1542-1406 print/1563-5287 online
DOI: 10.1080/15421406.2013.821646

Taylor & Francis
Taylor & Francis Group

Studies on Pressure-Dependent Electrical Resistivity of $MoSe_{2-x}Te_x$ Single Crystals

D. N. BHAVSAR* AND A. R. JANI

High Pressure Laboratory, Department of Physics, Sardar Patel University, Vallabh Vidyanagar, Gujarat, India

Electrical resistivity of 2H-$MoSe_{2-x}Te_x$ ($x = 0.25, 0.5, 1, 1.5, 1.75$) single crystals grown by chemical vapor transport technique have been measured in the pressure range 0.1–8 GPa. It is noticed that all these materials show a decrease in resistivity with increase in applied hydrostatic pressure. The materials become more and more metallic in nature as the pressure increases. The obtained results have been discussed in detail on the basis of energy band theory of semiconductors.

Keywords CVT method; electrical resistivity; high pressure; powder X-ray diffraction; single crystal; TMDCs

1. Introduction

Gapless graphene has limitations for its applications in nanoelectronics and nanophotonics which led to the finding of the 2D-materials with finite optical band gap such as BN, Transition Metal Dichalcogenides (TMDCs), and Transition Metal Oxides (TO_2). Depending on the interaction of transition metal and chalcogen orbitals, TMDCs offer a wide range of 2D-layered materials which have properties of metals, superconductors, Charge Density Wave (CDW) Systems, and Mott-insulators and semiconductors [1–9]. A single layer of TMDCs having stoichiometric of TX_2 like MoS_2, $MoSe_2$, $MoTe_2$, WS_2, and WSe_2 consists of a hexagonally arranged transition metal (T = Mo and W) sandwiched between two layers of chalcogen atoms (X = Se and Te). Within the layers, the metals and chalcogens form strong ionic–covalent bonds, while in bulk TMDCs, the layers are bonded by weak van-der Walls forces [10–13]. TMDCs like MoS_2, $MoSe_2$, $MoTe_2$, WS_2, and WSe_2 have emerged as promising materials for a range of applications. 2H-$MoSe_{2-x}Te_x$ ($x = 0.25$, 0.5, 1, 1.5, 1.75) TMDCs have been successfully synthesized in laboratory by chemical vapor transport technique [14] and their optical absorption and photoluminescence have been studied. These TMDCs 2H-$MoSe_{2-x}Te_x$ ($x = 0.25$, 0.5, 1, 1.5, 1.75) have semiconducting optical band gap in the range of 1.0–1.3 eV [15]. In order to use these materials as blocks in nanoelectronics, their electronic properties should be modified. Applied pressure offers a novel way of modifying the optical band gaps in terms of dc electrical resistivity measurement over a wide range. Some theoretical aspects of TMDCs show the semiconductor (S) to metal (M) transition for bilayers subjected to hydrostatic pressure.

*Address correspondence to D. N. Bhavsar, 106, High Pressure Laboratory, Department of Physics, Sardar Patel University, Vallabh Vidyanagar 388120, Gujarat, India. Tel.: +919429382908. E-mail: div.bhavsar@gmail.com, or janiar@rediffmail.com

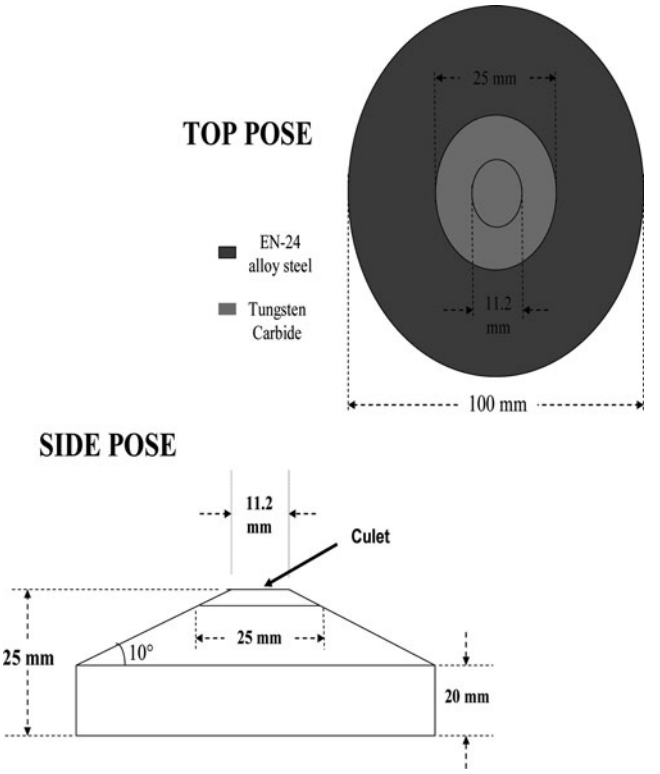

Figure 1. Typical anvil dimensions used in Bridgman opposed anvil apparatus.

2. Experimental Arrangement

The measurements of pressure-dependent in-plane resistivity of 2H-$MoSe_{2-x}Te_x$ ($x = 0.25$, 0.5, 1, 1.5, 1.75) single crystals were performed using Bridgman anvils pressed against each other by piston-cylinder-type hydraulic press. The Bridgman anvils consist of a tungsten carbide cylindrical piece, one face of which is ground in a tapered form ending with a flat anvil surface (culet). In a typical anvil, the anvil has a diameter of 100 mm, the WC cylinder is of 25 mm diameter with the culet surface of 11.2 mm diameter and the taper angle about 10°. The anvil face experiences high pressure but the material is heavily supported to prevent a failure. Thus, the anvil faces can support pressures in excess of 10 GPa. Typical anvil dimensions are depicted in Fig. 1.

Initially, a pyrophellite gasket of ∼150 μm thickness is fixed on the culet of anvil with epoxy. After that, the crater inside the gasket is filled by putting a disc of pressure transmitting medium (talk). The sample is directly placed on this disc and four wires are drawn above it as shown in Fig. 2. Then, another such gasketed anvil is placed on it. The whole assembly is pressed in a hydraulic press to generate high pressure. The generated pressure is measured by a fixed-pressure-point scale utilizing pressure-dependent electrical resistance of bismuth [16].

Using the described experimental arrangement, four-probe resistivity measurements were performed on 2H-$MoSe_{2-x}Te_x$ single crystals grown by chemical vapor transport

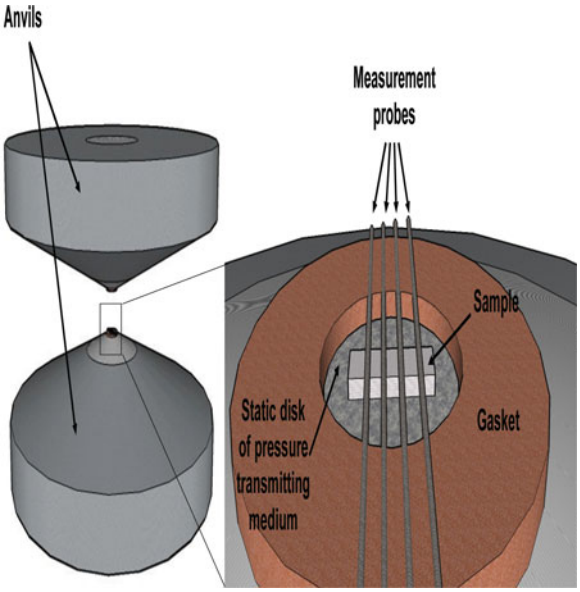

Figure 2. Arrangement of sample and probes in the pressure-dependent electrical resistivity measurement system.

technique. All the measurements were performed at room temperature up to 8 GPa. The obtained results are discussed in this paper.

3. Results and Discussion

Figure 3 shows the powder X-ray diffractograms of ternary 2H-$MoSe_{2-x}Te_x$ compounds. These diffractograms were thoroughly scanned for all the possible phases. It appeared from the powder X-ray diffraction patterns that there exists a quite good resemblance over the composition of Mo, Se and Te which leads to the results that arrangement of the Mo Se, and Te remains same as in the 2H-MoX_2 (X = S, Se and Te) structure. Thus, this compound may also be regarded as possessing layered structure with space group $p6_3/mmc$. In all the materials, 002 and 004 reflections are common indicating a strong preferred orientation along the c-axis. It was noticed that higher order reflections become broader related to the root mean square displacement of atoms from their mean positions indicating the presence of the disorder of the layer in this material.

From the obtained structural parameters, it is concluded that grown crystals of all compounds possesses 2H-polytype structure. Figures 4 and 5 show the variation of lattice parameters (a & c) and unit cell volume, respectively, with selenium proportion in 2H-$MoSe_{2-x}Te_x$ ($x = 0.25, 0.5, 1, 1.5, 1.75$) crystals.

The quality of a solid solution is usually examined from the composition-dependent lattice parameter changes in terms of the empirical Vegard's law [17,18]. This law states that, in the absence of strong electronic effects, the variation in lattice parameters with composition is linear in a true three-dimensional solid. The Vegard law is a consequence of the way a solid solution reduces strain by an expansion (or compression) when species of different sizes are involved. In a two-dimensional system, the non-Vegard's law behavior or, in other words, nonlinear changes in lattice parameter with composition have been well

Table 1. Structural parameters of 2H-$MoSe_{2-x}Te_x$ ($x = 0.25, 0.5, 1, 1.5, 1.75$) crystals

Crystals	$MoSe_{0.25}Te_{1.75}$	$MoSe_{0.5}Te_{1.5}$	MoSeTe	$MoSe_{1.5}Te_{0.5}$	$MoSe_{1.75}Te_{0.25}$
Coordination	Trigonal Prismatic Loop				
Space group	$P6_3/m\ m\ c$				
Unit cell parameters					
$a = b$ (Å)	3.494	3.446	3.314	3.304	3.293
c (Å)	13.862	13.812	13.204	12.998	12.941
Unit cell volume (Å^3)	146.5555	142.0423	125.5859	122.8817	121.5295

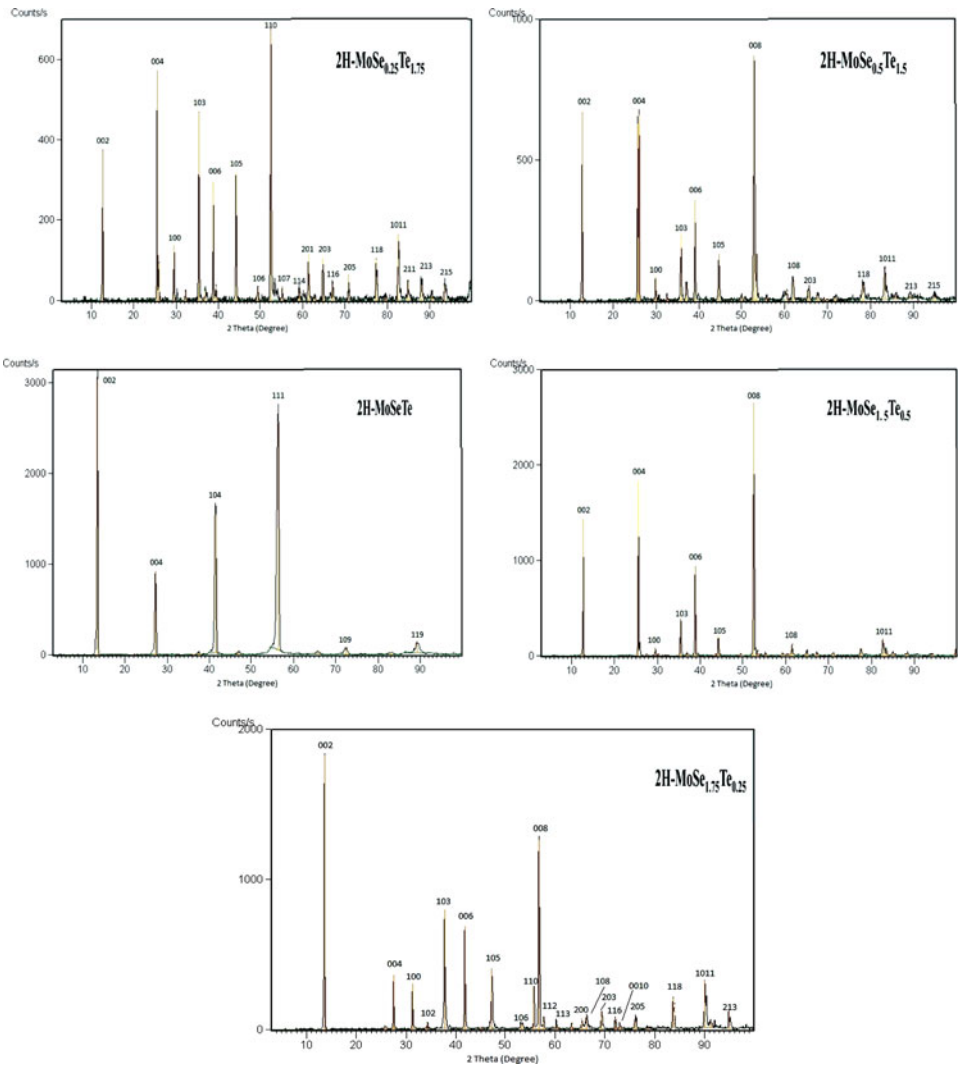

Figure 3. Powder X-ray diffractograms of 2H-$MoSe_{2-x}Te_x$ ($x = 0.25, 0.5, 1, 1.5, 1.75$) compounds.

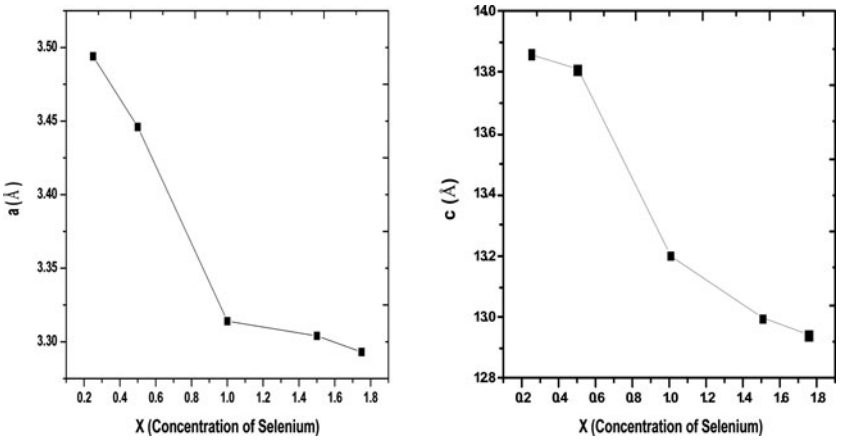

Figure 4. Variation of lattice parameters a & c (Å) with selenium proportion in 2H-$MoSe_{2-x}Te_x$ crystals.

documented [19–22]. The variations of lattice parameters (a and c) with the composition x shown in Fig. 4 indicate their decrement with increase in the selenium proportion. Finally, it results in decrement of unit cell volume with increase of selenium proportion in 2H-$MoSe_{2-x}Te_x$ crystals.

In all the materials, initially at low pressure, resistivity either increases or remains unstable. Above some value of pressure, it becomes stable and starts decreasing with

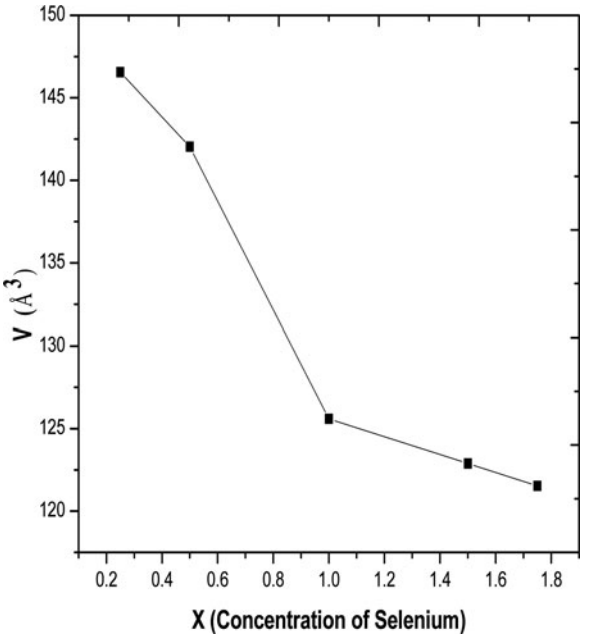

Figure 5. Variation of unit cell volume with selenium proportion in $MoSe_{2-x}Te_x$ ($x = 0.25, 0.5, 1, 1.5, 1.75$) crystals.

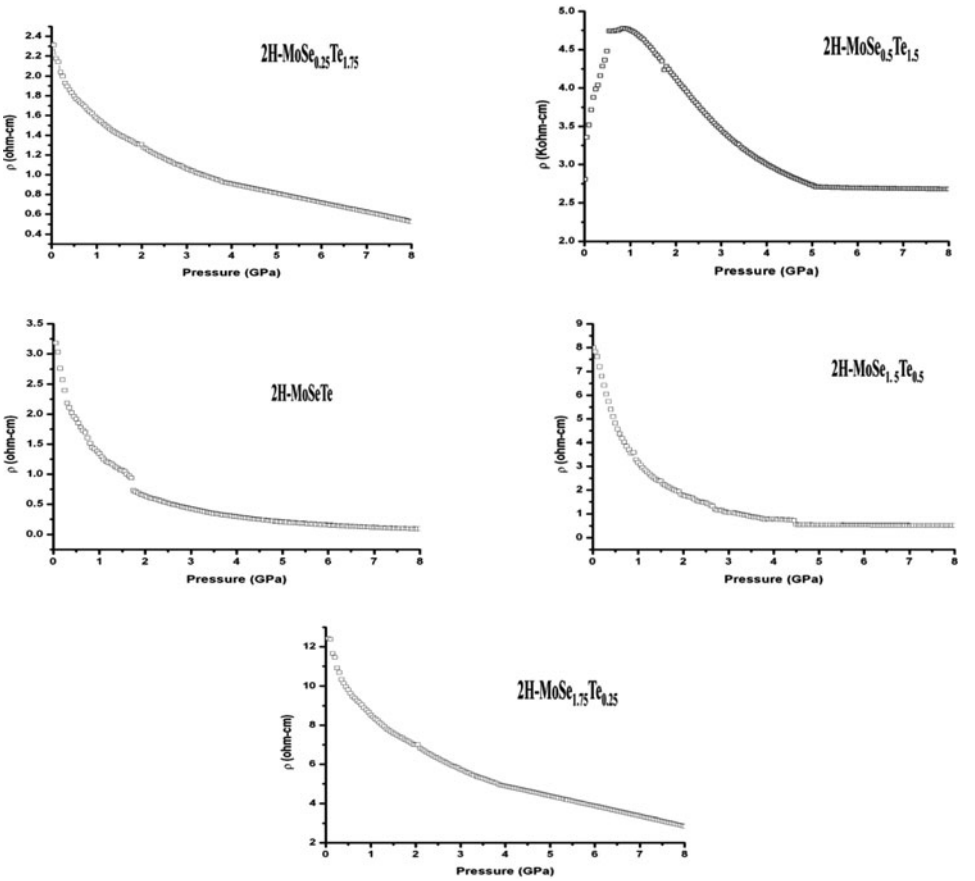

Figure 6. Pressure-dependent in-plane electrical resistivity of 2H-$MoSe_{2-x}Te_x$ ($x = 0.25, 0.5, 1, 1.5, 1.75$) crystals.

pressure in a regular manner. This always happens because, in this type of experiment, the measurement leads are only being placed on the sample meaning thereby that measurement leads are not being fixed to the sample. Because of this type of lead arrangement, initially the resistance of the contacts is high which gives the fluctuation in the measurements. Above this pressure (at some low pressure) when the measurement leads get proper pressure contact with sample, the results become steady.

The resistivity of all the materials is found to decrease with increase in pressure. Initially, it decreases rapidly with increase in pressure but the rate of change of resistance with pressure is found to change with pressure. Exact interpretation of the behavior of pressure-dependent resistivity of these materials can be constructed by considering some simple pictures of semiconducting conduction from band structure of $MoSe_2$ and $MoTe_2$ with applied pressure as under.

It is seen that the d.c. resistivity of the sample shows two different regions of behavior. In the low-pressure region of 0.4–2.20 GPa, the resistivity decrease is rapid, while in the region of higher pressure, the resistivity decrease is gradual. This transition onset for this sample is found to be in the region of 0.4–2.20 GPa. The resistivity decrease in the low-pressure region of 0.4–2.20 GPa may be due to the presence of the layered structure in these

type of TMDCs single crystals. The total density of states near the Fermi level reduces due to the shift of the conduction band maxima (CBM) and the valance band maxima (VBM) toward the Fermi level. By increasing the pressure, the contributions to the CBM from Mo-*d* and Se/Te-*p* orbital decrease, while Se/Te-*d* increase. The change in the resistivity as a function of pressure follows the same pattern for all the materials studied here. The change in the resistance as a function of pressure shows that all the materials became more and more metallic in nature at higher pressure. As the concentration of selenium is decreasing in 2H-$MoSe_{2-x}Te_x$, the semiconductor to metal transition occurring in the low-pressure region may due to the delocalization of the atomic orbitals. This leads to reduced interaction between metal and chalcogen atoms at lower pressure.

The slow decrements of resistivity with increase of pressure for all the compounds shows that the carrier mobility in the conduction band increases with pressure due to decrease in the intralayer bonds and shift from a two-dimensional material to a more three-dimensional material. The increase of carrier mobility of the conduction band is due to the contribution of carriers from the valence band [23].

Conclusions

In conclusion, we report the change in the resistivity of 2H-$MoSe_{2-x}Te_x$ as a function of applied pressure. The reduction of resistivity as a function of applied hydrostatic pressure may be caused by the interlayer interactions, which eventually lifts the degeneracies of bands and move them closer to the Fermi level. The decrease in the rate of change of resistivity with increasing pressure indicates the decrease in the compressibility of the sample under pressure. Furthermore, with increasing the pressure all the materials become more conducting means metallic nature is observed at high pressure.

Acknowledgment

The author D. N. Bhavsar is thankful to the DST for selection on INSPIRE Fellowship and for providing necessary financial support to carry out this work as a full-time Ph.D. student.

References

[1] Ding, Y., Wang, Y., Ni, J., Shi, L., & Tang, W. (2011). *Physica B*, *406*, 2254.
[2] Ayari, A., Cobas, E., Ogundadegbe, O., & Fuhrer, M. S. (2007). *J. Appl. Phys*., *101*, 014507-1.
[3] Morosan, E., Zandbergen, H. W., Dennis, B. S., Bos, J. W. G., Onose, Y., Klimczuck, T., Ramirez, A. P., Ong, N. P., & Cava, R. J. (2006). *Nat. Phys*., *2*, 544.
[4] Rossnagel, K., Seifarth, O., Kipp, L., Skibowski, M., Voβ, D., Kruger, P., Mazur, A., & Pollmann, J. (2001). *Phys. Rev. B*, *64*, 235119-1.
[5] Gabovich, A. M., Voitenko, A. I., Annett, J. F., & Ausloos, M. (2001). *J. Supercond. Sci. Technol*., *14*, R1.
[6] Hu, W. Z., Li, G., Yan, J., Wen, H. H., Wu, G., Chen, X. H., & Wang, N. L. (2007). *Phys. Rev. B*, *76*, 045103-1.
[7] Kusmartseva, A. F., Akrap, A., Berger, H., Forro, L., & Tutis, E. (2008). *Nat. Mater.*, *7*, 960.
[8] Kam, K. K., & Parkinson, B. A. (1982). *J. Phys. Chem*., *86*, 463.
[9] Han, S. W., Kwon, H., Kim, S. K., Ryu, S., Yun, W. S., Kim, D. H., Hwang, J. H., Kang, J.-S., Baik, J., Shin, H. J., & Hong, S. C. (2011). *Phys. Rev. B*, *84*, 045409-1.
[10] Sugai, S., & Ueda, T. (1982). *Phys. Rev. B*, *26*(12), 6554.
[11] Kam-Keung, Kam, Chi-Lan, Chang, & Lynch, D. W. (1984). *J. Phys. C: Solid State Phys*., *17*, 4031.

[12] Mattheiss, L. F. (1973). *Phys. Rev. B, 8*(8), 3719.
[13] Jaminson, W. E. (1972). *ASLE Trans*., *15*(4), 296.
[14] AlHilli, A. A., & Evans, B. L. (1972). *J. Cryst. Growth*, *15*, 93.
[15] Hong, Jiang. (2012). *J. Phys. Chem*., *116*, 7664.
[16] Patel, A. J. (2010). Ph.D. Thesis, Sardar Patel University, V.V. Nagar, India.
[17] Vegard, L. Z. (1921). *Phys. Rev. Lett*., *5*, 17.
[18] Vegard, L. Z., & Dale, H. Z. (1928). *Zeitschrift für Kristal*., *67*, 148.
[19] Whittingham, M. S., & Gamble, F. R. (1975). *Mater. Res. Bull*., *10*, 363.
[20] Dhanand, J. R., & Haering, R. R. (1981). *Solid State Commun*., 40.
[21] Sarfran, S. A. (1987). *Solid State Phys*., *40*, 183.
[22] Lee, S. (1989). *Phys. Rev. Lett*., *62*, 3066.
[23] Agarwal, M. K., Patel, S. G., & Chaki, S. H. (1992). *J. High Pres. Res*., *10*, 535.